Integrated tree canopy expansion and cool roofs can optimize air temperature and heat exposure reductions in Boston

Check for updates

Ian A. Smith [1] ✉, Dan Li [1], David K. Fork[2], Gregory A. Wellenius [3] & Lucy R. Hutyra [1,2]

Tree canopy expansion and albedo management represent pathways to reduce urban heat. Here we develop a statistical model to downscale coarse resolution estimates of air temperature and estimate marginal impacts of tree canopy and cool roof solutions across southern New England during 2021–2022. We quantify how tree canopy and cool roof solutions can be integrated to maximize heat exposure reduction, given feasibility and cost constraints. Afternoon estimates of air temperature cooling impacts from albedo and tree canopy cover fraction are −0.61 °C and −0.07 °C per increase of 0.1, respectively. Temperature reductions associated with tree canopy expansion are 35% higher than cool roofs, however, cool roofs on average provide higher heat exposure reductions due to implementation opportunities within dense, vulnerable regions of the city. Our Boston optimization identifies nearly twice as much area for cool roof implementation than tree canopy expansion. Cooling potential, implementation feasibility, and cost are critical considerations for identifying locally actionable, integrated climate solutions.

Global extreme heat exposure nearly tripled between 1983 and 2016[1] due to the combined effects of expanding populations and accelerated urban warming. Heat exposure in urban environments is exacerbated by combinations of non-reflective surfaces that absorb and retain heat during the day, reduced evapotranspiration due to impervious surface cover, and anthropogenic heat inputs from air conditioners and vehicles[2]. The consequences of extreme heat exposure include adverse health outcomes[3,4], increased energy demand[5], and diminished labor productivity[6], with disproportionate impacts borne by marginalized communities[7,8]. Cities have the potential to mitigate heat exposure by implementing measures that target modifications to the urban surface energy balance, such as expanding tree canopy and increasing albedo. Despite a considerable body of research estimating the effects of urban tree canopy and albedo management on various forms of heat[9–12] and emerging municipal ordinances around trees and cool roofs[13,14], policymakers lack integrated decision-making frameworks to empirically identify actionable, high-impact, solutions aimed at maximizing reductions in urban heat exposure. This analysis introduces a decision-making framework that identifies actionable solutions by applying spatial suitability rulesets and cost considerations to constrain potential increases in tree cover and albedo and quantifies the impact of potential solutions using heat exposure metrics, rather than air temperature changes alone.

Trees provide cooling benefits through evapotranspiration and shading. Urban tree canopies cast shade upon surface materials, reducing the amount of solar energy absorbed, stored, and reemitted by the built environment. Shade improves human thermal comfort by attenuating solar radiation that would otherwise transmit to the ground surface, reducing the real and perceived temperature by pedestrians[15]. Additionally, incoming solar radiation is absorbed by tree canopies for photosynthesis and liquid water is converted to water vapor, consuming heat and reducing the ratio of sensible to latent heat flux in the urban surface energy balance[16]. The cooling efficiency of urban trees varies as a function of background climate (e.g. solar irradiance intensity, background air temperature, background humidity), urban morphology (e.g. building geometry, road orientation), and tree traits (e.g. species, leaf area, size) with a wide range of reported cooling efficiencies across studies[17]. Numerical modeling simulations across a range of climate zones estimate the street tree cooling effects on air temperature to be between −0.05 °C and −1.4 °C per increase in tree cover fraction of 0.1 under clear sky summer afternoon conditions, with a median value of −0.3 °C per increase in tree cover fraction of 0.1[10]. Du et al.[18] used a network of weather station observations across Europe to estimate a range of urban tree cooling effects on air temperature between −0.01 °C and −0.1 °C per increase in tree cover fraction of 0.1 during afternoon conditions, with a mean value of −0.06 °C per increase in tree cover fraction of 0.1. A meta-analysis of 182 studies on the cooling effects of urban trees across 110 global cities reported mean temperature changes in pedestrian-level air temperature on summer days resulting from the implementation of trees with

[1]Boston University, Department of Earth & Environment, Boston, MA, 02215, USA. [2]Google LLC, Mountain View, CA, 94043, USA. [3]Boston University, Department of Environmental Health, Boston, MA, 02118, USA. ✉e-mail: iasmith@bu.edu

compact urban forms of −1.18 °C, −1.72 °C, −1.03 °C, and −1.31 °C in tropical, arid, temperate, and continental climates, respectively[17]. The impacts of tree canopy cover on urban air temperatures are scale-dependent with the strongest cooling effects observed at the scale of a typical city block (60–90 m)[19]. However, tree transpiration also increases urban humidity, potentially partially offsetting some or perhaps even all of the human health benefits provided by air temperature reductions[9]. Nonetheless, tree canopy expansion represents a potential pathway for reduced heat exposure in cities.

Surface albedo moderates the net solar radiation available to increase sensible heat fluxes and air temperature. In urban areas, albedo typically declines with increased impervious surface area and population density[20], contributing to the urban heat island effect and increased exposure of urban populations to high temperatures. Urban albedos can be managed to offset these impacts through the incorporation of reflective surfaces, such as cool roofs. We define cool roofs here as roofs designed to reflect more sunlight than a conventional roof through highly reflective, often white colored, materials and coatings. Estimates of the cooling effectiveness of bulk albedo changes on air temperature range from −0.2 °C to −0.9 °C (with a median cooling effectiveness of −0.6 °C) per albedo increase of 0.1 across a range of climate zones under clear sky summer conditions[10].

Numerous approaches have quantified urban heat and the associated cooling effectiveness of tree canopy and high albedo surfaces, each with its own set of tradeoffs. Computational fluid dynamics models and urban canopy layer models are physics-based, numerical approaches (E.g. ENVI-met, WRF[21,22]) to estimate urban surface and air temperatures and the influence of urban features at several scales with a high degree of experimental control. However, numerical simulations rely on imperfect representations of urban atmospheric processes, simplified urban form, and can be computationally prohibitive when implemented across large spatial domains. Other studies have leveraged spatially comprehensive, remotely sensed land surface temperature (LST) to estimate the sensitivities to landcover composition and characteristics[12,23]. LST analyses are advantageous in their ability to draw from long-term, high-resolution global datasets, but LST observations are not typically made at the warmest time of day. Moreover, the LST estimated from a sensor's point of view is likely a poor proxy of the air temperature perceived by humans and tends to be more sensitive to landcover impacts than air temperature[9,18]. Gridded spatial climate datasets (e.g. PRISM, Daymet[24,25]) provide estimates of air temperature by interpolating across ground-based weather station observation networks using statistical modeling techniques but are relatively coarse in both spatial and temporal resolution and do not capture the unique thermal properties of built environments. Machine-learning models trained on landcover data represent an emerging method for estimating urban air temperature[26,27], however, machine-learning models are optimized for prediction accuracy and the independent impacts of specific climate adaptation interventions can be difficult to interpret compared to statistical models such as linear regression.

This research introduces a straightforward statistical method for downscaling coarse-resolution regional models of air temperature that overcomes computational limitations associated with numerical modeling simulations and produces interpretable estimates of the marginal impact of urban cooling interventions. Furthermore, this work applies the model to demonstrate an integrated decision-making framework for allocating resources towards cool roofs or tree planting initiatives to maximize reductions in urban heat exposure. We describe a multiple linear regression modeling approach to downscale 1 km resolution gridded climate model estimates of air temperature from Daymet[25] to 200 m resolution air temperature estimates as a function of local landcover characteristics (tree canopy cover, albedo, and distance to water) and meteorological conditions (maximum daily air temperature, wind speed, and solar radiation). We utilize the regression approach to (1) estimate the marginal impact of tree canopy cover and albedo on afternoon air temperatures in urban environments across southern New England, United States (USA) and (2) consider how combinations of canopy and cool roof expansion can be

integrated to provide the highest reduction in population- and vulnerability-weighted heat exposure, given constraints on spatial feasibility (e.g. omitting areas not suitable for tree planting and roofs with low potential to support cool roofs) and the cost of solutions. We apply this modeling framework to estimate the impacts of tree canopy expansion and cool roof solutions on heat exposure in a scenario analysis for Boston, Massachusetts (MA), United States. Current heat exposure is estimated across June, July, and August (JJA) 2021 and 2022 using a vulnerability-weighted heat exposure index (VEI) that considers population density, population vulnerability (using a composite social vulnerability index[28]), and excess heat hours (hours above 24 °C) under current conditions of tree canopy extent and albedo. We estimate reductions in potential heat exposure by considering practical scenarios of tree canopy expansion and albedo modifications based on rulesets restricting the locations of implementation and a cost constraint equal to approximately 1% of Boston's annual operating budget. This framework allows for the identification of key locations for each heat mitigation solution considered, offering essential guidance for selecting climate interventions that yield the highest benefits within a fixed budget. While demonstrated in Boston, the statistical downscaling method and overall framework can be applied in other urban areas to derive the local marginal impacts of cool roof and tree cover interventions.

Results
Model evaluation and validation
We find strong agreement between observed and predicted air temperatures across all hours of day at validation weather stations (Fig. 1). Although data used to train the regression model come from a range of environments, both urban and rural, the validation data come from weather stations situated within urban settlements. The root mean square error (RMSE) of the regression modeling approach is 1.48 °C (Fig. 1). We observe little bias in observed versus predicted hourly air temperatures, with a slope of 1.00 and intercept of −0.02.

Figure 2 demonstrates the spatial model outputs across the modeling domain for a clear sky afternoon hour on June 20, 2022, at 15:00. The 200 m spatial resolution outputs of the regression model improve upon the 1 km spatial resolution of Daymet by a factor of 25. Most of the predictive capacity of the model comes from the inclusion of Daymet air temperature (Fig. 2B, C), which is not optimized for urban applications, but provide estimates of larger scale regional air temperature. Local scale variability (i.e. within 1 km Daymet pixels) in air temperature is accounted for in the additional model parameters of tree cover, albedo, wind speed, solar irradiance, and distance to the coast, which improve model prediction accuracy across all hours by 9% when compared to a regression model of the same form that only includes the Daymet air temperature (RMSE = 1.63 °C). The high spatial resolution, prediction accuracy, and consideration of fine-scale landcover impacts allows the regression model to downscale regional trends in air temperature to capture variability within highly heterogeneous urban ecosystems (Fig. 2B, C).

Albedo and tree cover cooling impacts
Afternoon air temperature was negatively related to tree cover ($p < 0.001$; Fig. 3A), with an estimated cooling impact from the regression model of −0.07 °C per increase in tree cover fraction of 0.1. Similarly, afternoon air temperature was negatively related to albedo ($p < 0.001$; Fig. 3B), with an estimated cooling impact from the regression model of −0.61 °C per increase in albedo of 0.1. All model coefficients are provided in Supplementary Table 1.

Spatial trends in heat exposure in Boston, MA
Mean population density in Boston was 3,080 people km^{-2}, ranging from 0 to 125,483 people km^{-2} (Supplementary Fig. 1A). Mean Social Vulnerability Index (SVI)[28] values were 0.5 and ranged from 0 to 1 where higher SVI corresponds to higher social vulnerability (Supplementary Fig. 1B). Mean JJA cumulative excess heat, defined as the sum of hourly afternoon excess heat for all hours > 24 °C, where excess heat is calculated as the estimated air
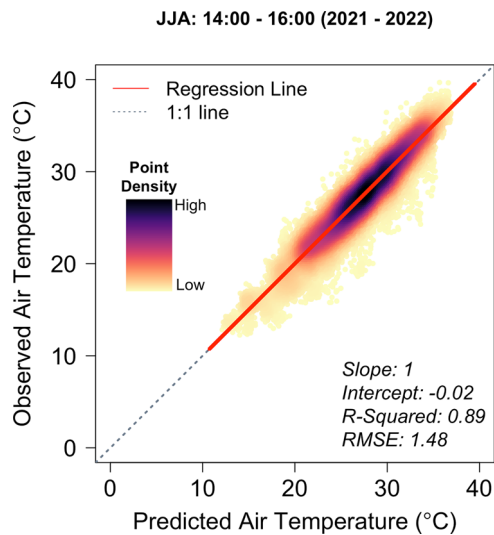
Fig. 1 | Air temperature model performance and validation. Observed air temperature (°C) at Weather Underground stations versus predicted air temperature (°C) for all afternoon (14:00–16:00) JJA hours. Darker colors correspond to a higher density of points.

temperature minus 24 °C, was 1052 °C hours > 24 °C and ranged from 918 to 1147 °C hours > 24 °C (Supplementary Fig. 1C). In general, the regions of the city with the lowest excess heat values coincide with the locations of forests and open green spaces, such as in Franklin Park and the Stony Brook Reservation in the center and southwestern areas of the city (Supplementary Fig. 1C). Conversely, the highest excess heat values are predominantly characterized by a high proportion of low albedo and impervious surfaces, such as the neighborhoods of Allston and Brighton in the northwest areas of the city (Supplementary Fig. 1C).

We find large spatial variability in the vulnerability weighted excess heat exposure index (VEI) across the city (Fig. 4A), where VEI combines excess heat with population density and SVI, with regions of concurrent high population density, high SVI, and high excess heat identified towards the central and northeast portions of the city. The southwestern portion of the city exhibits relatively low VEI values due to relatively low population density, low SVI, and low excess heat hours. This equal weighting scheme in the VEI balances the influence of the heat hazard, the human exposure, and social vulnerability. Several regions of the city have a high population density and excess heat, but low SVI resulting in a low VEI value (Fig. 4A).

Scenario analysis
We identify 19,719 buildings (2,852,799 m^2) suitable for conversion to a cool roof based on their low current albedo and roof slope (Supplementary Fig. 2;

Fig. 2 | Spatial air temperature model outputs. A Air temperature (°C) over the southern New England Domain on June 20, 2022, at 15:00. B Air temperature (°C) for the same hour in the Boston metro area compared to the Daymet maximum temperature for June 20, 2022 (C), with the heat exposure analysis domain highlighted in green. In all panels, red colors represent warmer temperatures, and blue colors represent cooler temperatures. Basemap data © Microsoft Bing Maps.
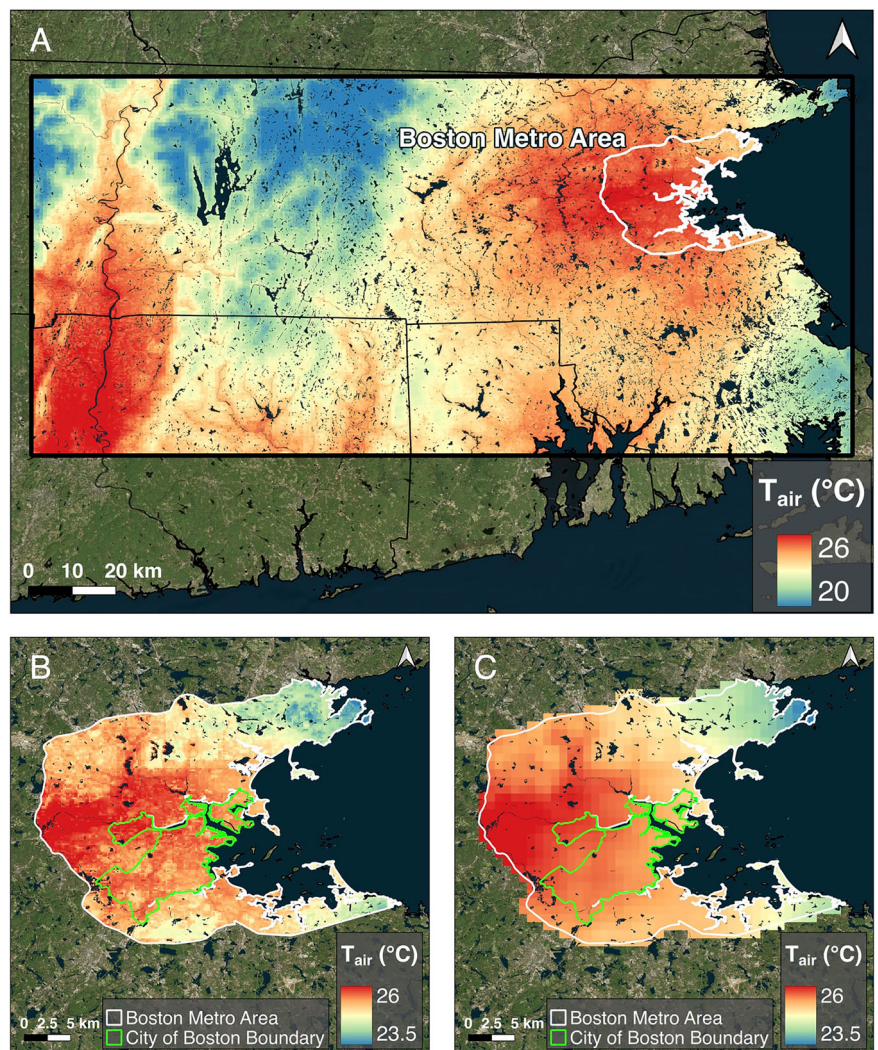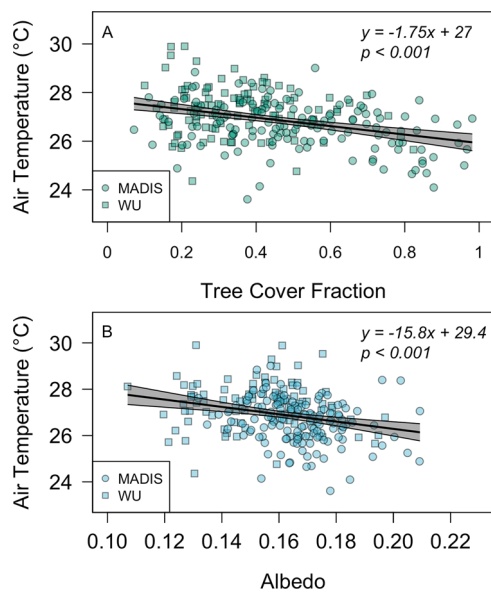
Fig. 3 | Afternoon air temperature variability across landcover characteristics. Mean 2021/22 afternoon (14:00–16:00) air temperature at each MADIS (circles) and Weather Underground (WU; squares) weather station versus **A** tree canopy cover fraction within 100 m of the weather station (green) and **B** albedo within 100 m of the weather station (blue). The gray shaded regions represent the 95% confidence interval of the linear regression.

see Methods section *Implementation of Cool Roof and Tree Canopy Expansion Scenarios*), representing 20% of the total buildings in the city. The estimated cost of converting all suitable roofs across the city is $199.6 M. We identify 23,012,450 m^2 of land suitable for the conversion to tree canopy cover in the city, representing 230,125 trees with an average crown area of 100 m^2 (Supplementary Fig. 2). The estimated cost of planting trees on all suitable land is $465.7 M. After applying the budget constraint of $34 M (based on the annual budget of the Boston Parks and Recreation Department; ~1% of the city budget) to identify the most impactful solutions, we identify 2976 buildings (412,664 m^2) to convert to cool roofs at a total cost of $28.9 M and 247,671 m^2 of land to convert to tree canopy (2477 trees) at a total cost of $5.0 M (Fig. 4A). Afternoon air temperature reductions within regions identified in the constrained solution range from −0.03 °C to −0.70 °C, with an overall mean afternoon air temperature reduction of −0.24 °C. The constrained solution would provide cooling benefits for nearly 80,000 Boston residents (approximately 15% of the total population when estimated from WorldPop), characterized by a median SVI value of 0.78 (mean SVI = 0.69) for a cost-effectiveness of $426 per person.

Fig. 4B zooms in to an example neighborhood (East Boston) located in the northeast part of Boston with high-impact solutions from the constrained scenario at the neighborhood scale in a three-census block area characterized by a high VEI. Within the neighborhood, we identify 0.1 km^2 of roof area to convert to cool roofs at an estimated cost of $6.8 M and 0.01 km^2 of tree canopy expansion at an estimated cost of $0.3 M. The neighborhood-level solutions are estimated to provide mean daily temperature reductions of up to −0.25 °C to approximately 11,000 residents characterized by an average SVI of 0.84 (Fig. 4C) for a cost-effectiveness of $632 per person.

Discussion

Cool roof and tree canopy climate adaptation strategies are both effective strategies to reduce urban heat. The afternoon cooling impact of albedo estimated here (−0.61 °C per increase in albedo of 0.1) is consistent with estimates from both numerical modeling studies and other observational studies. Reviews of the numerical modeling literature report mean afternoon albedo air temperature cooling impacts of −0.9 °C per increase in albedo of 0.1[11] and median impacts of −0.6 °C per increase in albedo of 0.1[10]. Mohegh

et al.[29] implement a regression modeling approach to estimate afternoon albedo air temperature cooling impacts of −0.2 °C per increase in albedo of 0.1 in the San Fernando Valley in California, USA. The afternoon cooling impact of urban tree cover estimated here (−0.07 °C per increase in tree canopy fraction of 0.1) is within the range of reported effects from numerical modeling studies (−0.05 °C to −1.4 °C per increase in tree cover fraction of 0.1) and consistent with other observational studies (mean of −0.06 °C per increase in tree canopy fraction of 0.1)[18], albeit lower than most estimates from numerical modeling studies (median of −0.3 °C per increase in tree canopy fraction of 0.1)[10].

We find similar spatial patterns in air temperature versus LST (Supplementary Fig. 3) but note substantial differences in the sensitivity of LST and air temperature to changes in tree canopy cover and albedo. The magnitude of the air temperature albedo cooling effects estimated in this study is approximately one-third of the magnitude of LST albedo cooling effects estimated for the City of Boston (−1.89 °C per increase in albedo of 0.1)[12]. The magnitude of the air temperature tree cover cooling effects estimated in this study is approximately 9% of the magnitude of LST tree cover cooling effects estimated for the City of Boston (−0.8 °C per increase in tree fraction of 0.1)[12], consistent with other reported air temperature/LST sensitivity ratios of 8% and 11%[9,18]. Our results are also in agreement with the study by Chakraborty et al.[9], which observed weaker associations between urban greenspace and air temperature than for urban greenspace and LST and even weaker associations between urban greenspace and the heat index. The reduced sensitivity of air temperature to landcover characteristics, compared to that of LST, is attributed to the mixing power of atmospheric turbulence. While air temperature is a more relevant metric of heat exposure than LST, other factors such as incoming solar radiation, humidity, and wind speed also impact heat stress in urban environments[30], which are not considered here in our work. For example, increases in evapotranspiration associated with tree canopy expansion can increase atmospheric moisture, potentially offsetting a portion of the cooling benefits from air temperature reductions when considering the impact of canopy expansion on moist heat stress[31].

The calculated cooling effectiveness of albedo and tree canopy solutions represent only one dimension of urban heat mitigation considerations. Of equal importance is the potential to implement these solutions when considering spatial constraints associated with the current built environment. We also observe that it is much more feasible to find space for planting trees to yield a 0.1 increase in cover fraction than it is to increase the albedo by 0.1 using cool roofs. For all 200 m grid cells in Boston with tree planting opportunities, we estimate a mean potential tree fraction increase of 0.19, corresponding to an afternoon temperature reduction of −0.13 °C. In contrast, for all 200 m grid cells in Boston with cool roof opportunities, we estimate a mean potential albedo increase of 0.014, corresponding to an afternoon temperature reduction of −0.09 °C. For both solutions, we identify grid cells with potential afternoon temperature reductions of up to −0.7 °C, representing areas with either large areas of natural ground suitable for tree canopy expansion or many flat, dark rooftops suitable for conversion to cool roofs.

The higher frequency of cool roof solutions compared to tree canopy solutions selected in the constrained optimization scenario within Boston is a product of solution proximity to vulnerable populations, rather than the cost of solutions. Our optimization analysis identifies approximately 0.41 km^2 of roof area for conversion to cool roofs in Boston, compared to approximately 0.25 km^2 of tree canopy expansion. The higher proportion of building solutions versus tree canopy solutions is driven by the proximity of building solutions to densely populated regions where heat exposure is highest. For example, the average population density of all 200 m grid cells with opportunities to expand tree canopy cover is 3235 people km^2 compared to an average population density of 5494 people km^2 in grid cells with cool roof conversion opportunities. We find that the higher frequency of selected cool roof solutions relative to tree canopy expansion solutions is not sensitive to the cost of solutions. For example, if the unit cost of cool roof implementation is doubled and the unit cost of tree planting is halved, we

Fig. 4 | Integrated heat exposure reduction solution from constrained optimization. A Optimal integrated solution to maximize reductions in vulnerability-weighted population excess heat exposure constrained by a budget of $34,080,037 overlaid on the vulnerability weighted excess heat exposure index (red) in Boston, MA, where green symbols represent tree canopy expansion and blue symbols represent cool roof implementation. **B** Optimal integrated solution for a high impact region in East Boston. **C** Mean estimated air temperature reduction (°C) across all hours in JJA associated with the constrained, integrated solution, where darker colors represent a stronger cooling effect. Basemap data © Esri and contributors.
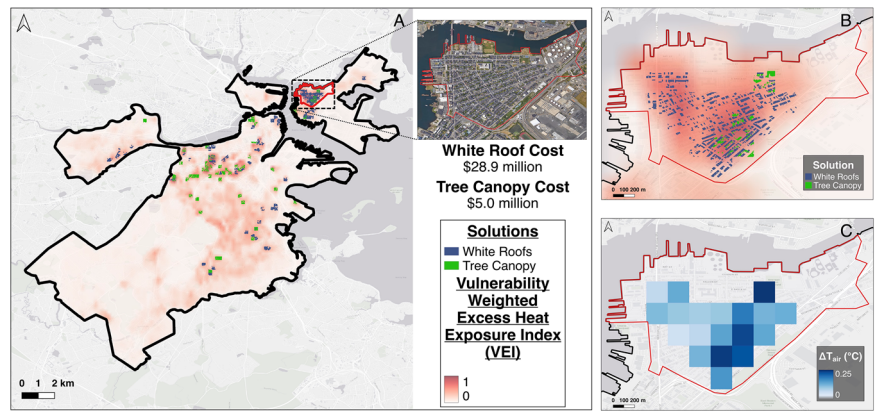
identify fewer overall solutions due to the higher cost of cool roof implementation, but still identify more cool roof opportunities (0.23 km²) than tree canopy expansion opportunities (0.09 km²) due to the higher availability of building solutions in density populated areas. Therefore, climate adaptation strategies with a focus on reducing heat exposure should not only consider the potential magnitude of air temperature reductions, but also the availability of space to implement solutions that reduce air temperatures in high population density areas. At a higher cost, space for tree canopy expansion could be created by installing tree pits on currently paved surfaces, such as sidewalks, which may increase the heat exposure reduction potential of tree planting in highly urbanized areas. More extensive changes in the urban form can allow for far greater expansion of the tree canopy, as exemplified by the development of superblocks in Barcelona[32], but doing so may be prohibitively expensive and politically challenging.

The magnitude of potential air temperature reduction does not necessarily correspond to the magnitude of reduction of heat exposure experienced by people. An extensive body of literature demonstrates that days of moderate and extreme heat are associated with higher risk of death and illness[33]. Population vulnerability to extreme heat varies substantially within as well as between cities[34], and the most effective heat adaptations will focus on those neighborhoods within a city with the greatest potential for health benefits. Specifically, to the extent that the goal of reducing air temperature is to protect public health on hot days, the most effective cooling interventions will be those targeted to areas of the city at the intersection of high population density, high heat conditions, and high vulnerability to the adverse health impacts of heat. The VEI we used here provides one simplified approach to identify those neighborhoods where reductions in ambient temperature are likely to have the greatest benefit on population health. Our modeling framework could be extended to directly estimate, under various assumptions, the health benefits of different cooling adaptations in terms of tangible benefits to population health such as the number of deaths or emergency department visits averted.

In practice, climate adaptation strategies often aim to provide multiple simultaneous benefits to communities, many of which are not considered in this analysis. Urban trees provide numerous co-benefits to urban communities such as improving physical and mental health[35,36] and facilitating social cohesion[37]. In contrast, cool roof solutions are largely targeted towards temperature regulation and reducing building energy demand[38], with fewer co-benefits. The allocation of resources to cool roof solutions versus tree canopy solutions would likely shift substantially if multiple benefit criteria were considered beyond reducing heat exposure, highlighting a simplification of the decision-making framework implemented here.

This analysis omits several important cost considerations from the implementation of solutions, including long-term maintenance and time to realize the putative benefits. The City of Boston estimates annual tree maintenance costs of $896.30 per tree, including the costs associated with pruning, pest/disease treatment, and end-of-life removal[39]. When maintenance costs are considered, the initial planting investment of $5.0 M for

2477 trees (0.25 km⁻²) estimated in the constrained, integrated scenario would increase to $27.2 M over a ten-year period, or $10.9 M km⁻² yr⁻¹. In comparison, the ten-year annualized cost of the cool roof solutions identified in the constrained, integrated scenario would amount to $7.0 M km⁻² yr⁻¹, assuming no roof maintenance or cleaning over the ten-year period. Both solutions could potentially reduce costs associated with building cooling during the summertime, however, the time required to achieve cooling benefits differs across solutions. Cool roofs provide the maximum amount of cooling benefits at the time of implementation when the albedo is highest. Over time, the accumulation of dirt and pollutants reduces the reflectivity of the rooftop, leading to an observed decline in albedo and the associated cooling benefits over time in the absence of cleaning[40]. Conversely, urban trees provide relatively few benefits in the early stages of their life with cooling benefits increasing over time until reaching maturity[41]. Our analysis describes a framework for identifying the locations of high impact heat adaptation solutions targeting heat exposure reductions in cities but does not consider the net benefits over the full life cycle of cool roofs and trees.

The modeled albedo change from cool roof implementation in this analysis is estimated using the observed albedo of currently cool roofs in Boston. The mean albedo of currently flat, dark roofs in Boston is 0.12 (σ = 0.02). The flat, dark roof albedos are modified in the cool roof scenario by sampling from the distribution of observed cool roof albedo, with a mean albedo of 0.45 (σ = 0.15). The mean albedo assigned to flat, dark rooftops is consistent with ENERGY STAR program requirements for roof products, which require a flat roof albedo of at least 0.5 three years after installation[42]. As roof coating technology advances, higher albedo products with more resistance to pollutant accumulation may increase the potential albedo change and cooling benefits associated with cool roofs.

In the tree canopy expansion scenario, individual tree crown area is assumed to be 100 m², which is an overestimate of the crown area for newly planted saplings and underestimate of the crown area for fully mature open grown trees[43,44]. As the City of Boston typically plants young trees with an average diameter at breast height (DBH) of 7.6 cm, the cooling effects resultant from tree canopy expansion estimated here would not be achieved for several years, assuming the survival of all trees. Therefore, the tree cooling impacts estimated from tree canopy expansion, which assume that impacts are fully effective immediately, are overestimates during the early stages of tree lives, however, trees could potentially provide more benefits than estimated here in the later stages of their lives if their tree crowns surpass the 100 m² area estimated here.

This analysis does not consider property ownership and identifies climate adaptation solutions on private property where municipalities have limited opportunities for implementation. The exact buildings and locations identified for tree canopy expansion may not be feasible for cities to directly intervene, however, cities may be able to employ alternative strategies for promoting cool roof or tree canopy adoption in targeted neighborhoods. Cool roof incentive programs offer subsidies, rebates, or loans to

homeowners and businesses to encourage cool roof installations on residential and commercial properties. Such incentives could be promoted as part of existing energy efficiency incentive programs. When tree planting opportunities are identified in residential or commercial lawns, cities may consider targeting nearby public sidewalks to install new tree pits as an alternative method to increase tree canopy cover in priority neighborhoods.

The regression model framework described in this analysis allows for regional parameterization to account for differences in air temperature sensitivity to landcover/albedo across climate zones. The model developed here for the temperate, moist climate of southern New England would likely lose predictive power when applied in different climate zones which may require distinct coefficients to capture the cooling impacts of tree canopy and albedo. The datasets used in this study are available across the USA allowing for location-specific parameters to be derived. In this way, variability in the cooling impacts of climate adaptation strategies across climate zones can be explored at scale. Model performance across a diverse assemblage of cities is beyond the scope of this analysis and requires further exploration to quantify model performance outside of southern New England.

Our results support the use of a straightforward, statistical modeling framework to derive estimates of cooling impacts from the climate adaptation strategies of tree canopy expansion and albedo management. The cooling impacts estimated here are within the range of reported impacts from numerical modeling studies, with the additional benefit of feasible model applications across large spatial domains and time periods. We demonstrate how tree canopy expansion and cool roof solutions can be integrated to maximize heat exposure reductions in urban areas given reasonable spatial and cost constraints. When applying the model in Boston, we find the most impactful solutions for reducing vulnerability-weighted population heat exposure are those found near densely populated, socially vulnerable areas. Due to the spatial distribution of dark, flat roofs suitable for cool roofs and impervious surfaces not suitable for tree planting in Boston, we identify nearly twice as much area for cool roof interventions than tree canopy expansion to maximize heat exposure reductions, however, the balance of solutions likely varies across cities as a function of the air temperature cooling potential of solutions, the feasibility of implementation, population characteristics, and cost of solutions.

The modeling approach and decision-making framework demonstrated here has the potential to provide critical information on the local effectiveness of popular heat exposure reduction solutions rapidly being adopted by cities and can estimate spatial variability in the potential of solutions to reduce heat exposure, increasing the efficiency of resource allocation for heat adaptation. The model alone does not, however, provide a comprehensive pathway towards climate resilience due to several simplifications and limitations. This analysis solely targets the heat benefits of solutions, relies on simplified unit costs, does not consider a full life cycle assessment of solution costs and benefits, and simplifies the timeline of expected benefits. Despite these simplifications, the modeling framework serves as a starting point for policy makers to make informed decisions about the types and locations of interventions most relevant to their city. As cities work to address the challenge of rising temperatures and heat exposure, future investigations should explore regional variability in climate solution cooling impacts, quantify the impacts of climate adaptation on moist heat stress, consider the co-benefits of various solutions over their entire life cycle, and translate heat exposure reduction impacts to impacts on public health and well-being.

Methods
Study domain
The spatial domain of this analysis spans over 20,000 km², including five major urban areas: Boston, MA, Worcester, MA, Springfield, MA, Hartford, CT, and Providence, RI (Supplementary Table 2). The region is characterized as a mesic, continental climate with warm summers and no dry season[45] where the non-built-up land between urban centers is primarily composed of forests, wetlands, and croplands[46].

Data for regression model
To estimate the cooling impacts of each heat mitigation solution, we relate hourly observations of afternoon air temperature from a weather station network in southern New England, USA to coarse resolution models of regional daily maximum air temperature, hourly wind speed, hourly solar irradiance, proximity to the coast, and the proximate tree canopy cover and albedo near the weather stations. Our modeling framework produces a linear model to estimate hourly air temperature during afternoon hours (14:00–16:00 local time) as a function of landcover composition at 200 m spatial resolution across a range of urban forms. This analysis focuses on afternoon air temperatures to capture the impact of cool roof and tree cover interventions when daytime temperatures are highest, the urban boundary layer is well-mixed, and air temperature urban heat island effects are smallest. We validate the modeling approach using a second, distinct observational network of weather stations concentrated in the urban areas.

Air temperature training and validation data
Weather station temperature data from the Meteorological Assimilation Data Ingest System (MADIS) for June, July, and August (JJA) 2021 and 2022 were used to train the regression model[47]. Hourly observations were initially filtered by MADIS quality control (QC) flags indicating verified observations. After QC filtering, stations were further filtered by observation frequency wherein we required a minimum of 80% of JJA hours in both 2021 and 2022. Stations with more than 5% water cover within 100 m of the stations were removed from the dataset. The locations of the remaining 139 MADIS stations with valid hourly air temperature time series during JJA 2021 and 2022 were buffered by 100 m to quantify the proximate landcover composition and albedo (Fig. 5A, B). The 100 m buffer size was determined based on the estimated scale of urban tree canopy cooling impacts of 90 m[19] plus 10 m to account for uncertainty in GPS estimates of exact weather station locations.

Observational air temperature data from the Weather Underground network[48] were used to validate the regression model. For each of the five cities in the spatial domain, hourly air temperature observations were acquired for all Weather Underground stations within a 5 km buffer of the city (Fig. 5A). We applied the same QC protocols to the Weather Underground stations, resulting in 153 stations.

Regression model development and validation
Our approach to modeling more granular urban air temperature includes broadscale weather inputs as well as local scale landcover characteristics to calculate the impact of tree canopy cover and albedo (Supplementary Table 3). We fit a multiple linear regression model ($R^2 = 0.86$, $p < 0.001$, RMSE = 1.67 °C) corresponding to afternoon hours to estimate air temperature at hour i as:

$$\begin{aligned}
T_{air,i} = \beta_0 + \beta_1 \times Tree + \beta_2 \times Albedo + \beta_3 \times Wind_i + \beta_4 \times Solar_i \\
+ \beta_5 \times Distance_{water} + \beta_6 \times T_{max} + \beta_7 \times Hour + \beta_8 \times Hour^2
\end{aligned}$$
(1)

T_{air} (°C) represents the observed air temperature at the MADIS weather stations. Tree is the 100 m buffered weather station fractional tree canopy cover from the Google panoptic landcover dataset[49]. Albedo is the 100 m buffered weather station albedo from Sentinel-2, derived from the Bonafoni & Sekertekin[50] narrow-to-broadband algorithm for 2021 and 2022 cloud-free summertime mean albedo composites. Wind (m s⁻¹) is the 13 km, hourly Rapid Refresh (RAP) wind speed[51] at each weather station. Solar (W m⁻²) is the 0.05°, hourly Geostationary Operational Environmental Satellite (GOES) surface solar irradiance[52]. Distance$_{water}$ (m) is the calculated shortest Euclidean distance between each weather station and the coastline. T_{max} (°C) is the Daymet[25] 1 km estimated maximum daily temperature. Hour represents the hour of day (14:00, 15:00, or 16:00 local time). A correlation table between model inputs and air temperature is provided in Supplementary Table 4. The model does not account for other urban
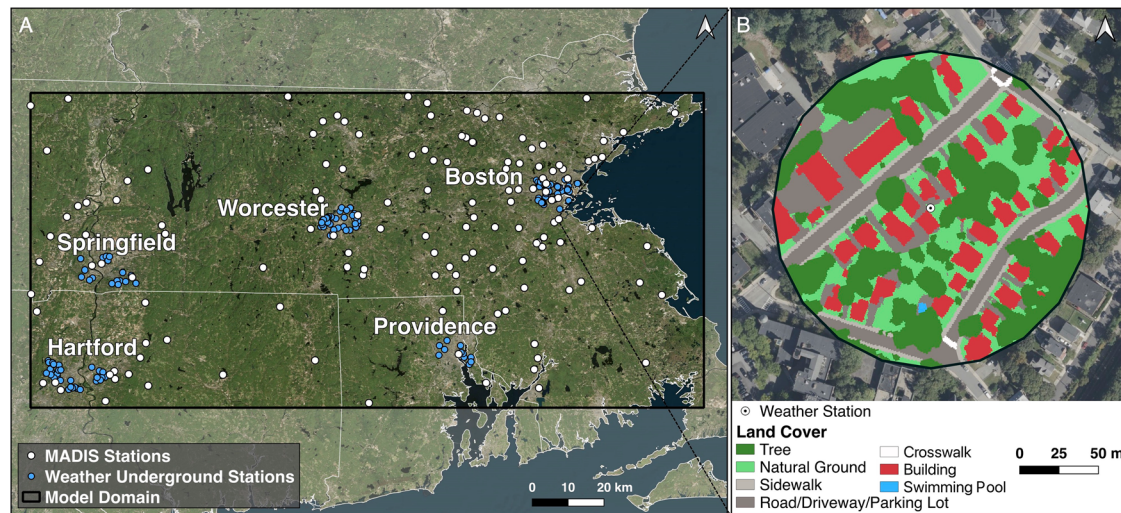
Fig. 5 | Model spatial domain and weather station buffers. A Locations of MADIS weather stations (white) used to train the model ($N = 139$) and Weather Underground stations (blue) used to validate the model ($n = 153$). **B** Example of high-resolution landcover data within 100 m buffer of a MADIS weather station in Boston, MA. Basemap data © Microsoft Bing Maps.

features that are known to influence local air temperatures such as urban geometry or anthropogenic heat inputs.

The regression modeling approach was validated by predicting hourly air temperatures at 153 urban weather stations from the Weather Underground weather station network and quantifying model bias and prediction accuracy statistics. We conducted an additional within-sample validation exercise by (1) randomly selecting 70% of MADIS weather stations to train the model ($N = 97$) and 2) predicting hourly air temperatures at the remaining 30% of MADIS weather stations ($N = 42$; Supplementary Fig. 4). All regression modeling and statistics were conducted using R version 4.4.1[53].

Given the widespread application of machine learning techniques for similar applications, we compared the performance of the regression modeling approach to a random forest and Extreme Gradient Boosting (XGBoost) modeling approach using the same independent variables. All three methods shared similar performance indicators when validated with the Weather Underground weather station network, with root mean square errors of 1.48 °C, 1.42 °C, and 1.32 °C for the regression, XGBoost, and random forest models, respectively. We opt to use the linear regression model in this analysis due to similar performance metrics across model types, the linear relationships observed between air temperature and independent variables (Fig. 3A, B), and the simple interpretation of marginal impacts provided by the regression model coefficients.

Model application

We apply the regression modeling framework to estimate the impact of tree canopy expansion and surface albedo modifications via cool roofs in Boston, MA to demonstrate the model utility in a decision support framework. We created a vulnerability weighted population excess heat exposure index (VEI) to summarize factors contributing to population demand for cooling[54] by equally weighing population density (WorldPop Global Project Population dataset)[55], social vulnerability (Centers for Disease Control and Prevention and Agency for Toxic Substances and Disease Registry Social Vulnerability Index; SVI)[28], and cumulative excess heat across a 200 m spatial resolution grid to approximate the 200 m diameter of the weather station buffers. The SVI combines 16 census variables to summarize socioeconomic status, household characteristics, racial and ethnic minority status, and housing type to characterize the impact that hazards and stressors may have on communities. The VEI allows us to estimate spatial variability in cooling demand[54] under current conditions (baseline) and scenarios of potential tree canopy expansion and cool roof conversion.

Cumulative JJA excess heat (°C hours > 24 °C) was estimated by applying Eq. (1) across the 200 m grid to estimate the air temperature within each grid cell for each afternoon hour in JJA 2021 and 2022 under current conditions of tree canopy cover and albedo. The excess heat threshold was set at 24 °C, representing a typical set-point temperature for air-conditioning use[56,57]. For estimated hourly temperatures greater than 24 °C, hourly excess heat was calculated as the estimated air temperature minus 24 °C. The excess heat threshold may be expected to vary across population characteristics such as age and activity level, however, we choose to use a fixed threshold here as the combination of excess heat with SVI is expected to capture variability in social vulnerability to excess heat conditions. Cumulative excess heat degree hours for each grid cell and each year were calculated as the sum of hourly afternoon excess heat during JJA, with a baseline excess heat estimate calculated as the mean cumulative afternoon excess heat value for each grid cell across 2021 and 2022.

Baseline population heat exposure was estimated by combining population density, vulnerability, and excess heat values for each 200 m grid cell as:

$$VE_{baseline} = \text{Population Density} \times SVI \times \text{Heat Excess} \quad (2)$$

where $VE_{baseline}$ represents vulnerability weighted excess heat exposure (people °C hours > 24 °C km^{-2}) under current conditions of tree canopy cover and albedo. VE was normalized to an index ranging from zero to one as:

$$VEI_i = \frac{VE_i - \min(VE)}{\max(VE) - \min(VE)} \quad (3)$$

where VEI_i represents the vulnerability weighted excess heat exposure index for grid cell i, VE_i represents the vulnerability weighted excess heat exposure for grid cell i, $\min(VE)$ is the minimum VE across all grid cells, and $\max(VE)$ is the maximum VE across all grid cells.

Implementation of cool roof and tree canopy expansion scenarios

There are countless possible scenarios for urban heat mitigation that can optimize various combinations of low cost, ease of implementation, high temperature reduction, or health risk reduction in specific communities among many other possible goals. For this demonstration, we focus on the potential for low-slope roof albedo increases and tree planting in pervious

**Fig. 6 | Identification of potential cool roof implementation and tree canopy expansion.**
A Example of building classification within a 200 m grid cell demonstrating the selection of flat, dark roofs to modify. Other roofs represent building types not considered such as sloped roofs and sheds. **B** Demonstration of modified albedo's applied to flat dark roofs to estimate the new cool roof albedo. **C** Current landcover composition and locations of empty tree pits (blue stars). **D** Demonstration of tree canopy potential where natural ground >2 m from buildings and empty tree pits represent opportunities for tree canopy expansion (Potential Tree). Basemap data © 2025 Google.
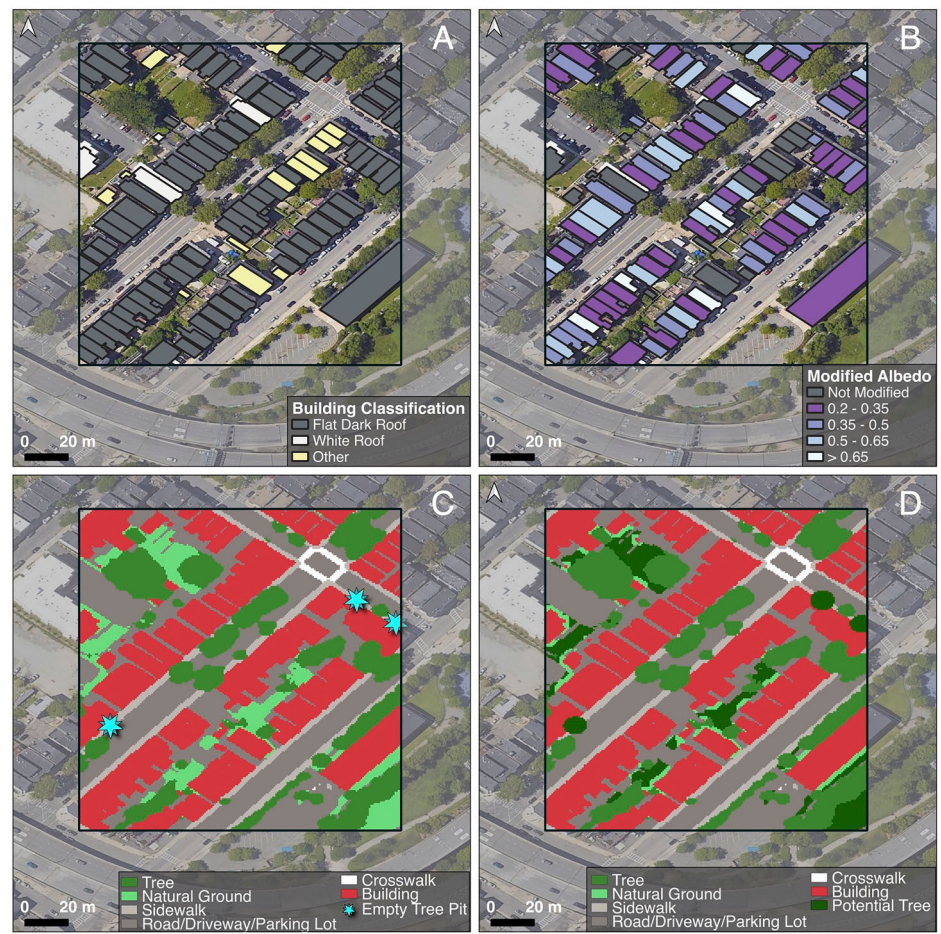
areas to reduce VEI within a constrained budget. Other interventions are possible, including modifying the albedo of high-slope roofs, walls, and sidewalks to create cool surfaces or adding trees via the removal of paved surfaces (sidewalks, parking lots, etc.). To find suitable locations for cool roof interventions in Boston and carry out cool roof implementation scenarios, we (1) identify all buildings with flat roofs that are not currently cool roofs, (2) quantify the albedo distribution of all existing cool roofs in Boston, and (3) assign a new albedo to all buildings with flat roofs that are not currently cool roofs based on the distribution of existing cool roofs. To find suitable locations for tree canopy expansion in Boston and carry out tree planting scenarios, we 1) identify empty street tree pits and pervious areas that are not classified as tree canopy and do not interfere with buildings and 2) replace the existing landcover with tree canopy.

We incorporate local data on roof structure and current roof albedo to constrain the locations of potential cool roof interventions (Fig. 6A). Suitable locations for cool roof implementation were defined as buildings with dark, flat rooftops. Flat, cool roofs typically yield higher albedos than sloped roofs due to their ability to reflect incoming solar radiation from a larger proportion of their total area at a wide range of solar angles. Furthermore, existing cool roof incentive programs often require roofs to be flat as a program qualification. Flat roofs in Boston were identified by combining the Boston buildings inventory[58], which delineates the outlines of rooftops within the city, with property assessment data[59], which classifies building roof structure.

Existing cool roof albedos were calculated as the pixel area-weighted mean albedo of each roof polygon during JJA 2022. Mean roof albedos were manually inspected to determine an albedo of 0.2 as a threshold to indicate the presence of a cool roof (Supplementary Fig. 5), where roofs with albedos less than 0.2 were assumed to be dark. Given that urban roof segments are small and are likely to include mixed land use pixels, we estimated a current

distribution of cool roof albedos by calculating the maximum pixel albedo value for each cool roof after buffering the roof polygon by −10 m to reduce the influence of mixed pixel reflectivity on cool roof albedo (Supplementary Fig. 6). This cool roof albedo distribution was subsequently sampled from in the scenario analysis to assign new roof albedos to buildings classified as suitable for cool roof interventions (Fig. 6B).

Potential suitable locations for tree canopy expansion were defined as areas of natural ground cover without trees that are located greater than 2 m from buildings and empty street tree pits (i.e., existing tree pits without trees; Fig. 6C)[60]. Due to the higher costs associated with tree planting within currently paved areas[39] and additional spatial restrictions related to the creation of new tree pits, such as minimum sidewalk width and minimum distances from infrastructure such as fire hydrants and light poles, this study did not consider tree planting opportunities requiring the creation of new tree pits.

Scenario analysis

To estimate the temperature reductions associated with converting dark, flat roofs to cool roofs we increased the albedo value of all buildings identified as having dark, flat rooftops and recalculated the *VE* by estimating hourly cumulative afternoon excess heat for JJA 2021 and 2022 for each 200 m grid cell under the increased albedo conditions. Rooftop albedos values were increased by randomly sampling from the observed cool roof distribution for Boston (Supplementary Fig. 6; Fig. 6B). This is a conservative cool roof albedo estimate reflecting typical aged values, including the darker elements on roofs such as heating, ventilation, air conditioning systems and skylights, where new coating technologies could yield higher albedos. The impact of increased building albedos on 200 m grid cell albedos was estimated by computing an area weighted mean albedo value for each grid cell based on the newly assigned building albedos and the pixel area weighted mean albedo of the grid cell fraction that was not modified.

The potential impact of tree canopy expansion was estimated by replacing the categorized landcover raster values in all pixels designated as suitable for tree canopy expansion with tree cover and recalculating the *VE* by estimating hourly cumulative afternoon excess heat for JJA 2021 and 2022 for each 200 m grid cell under the increased tree cover conditions. All natural ground pixels greater than 2 m from buildings were replaced with tree cover. In empty street tree pits, we created 5.6 m buffers around the centroid of each tree pit to create 100 m^2 circles, representing a reasonable tree crown area for commonly occurring urban street tree species[43,44]. We chose to represent mature open grown tree canopies to represent the eventual cooling from trees, but it would require years for a tree to attain such a size. Each landcover pixel within the 100 m^2 buffers was replaced with tree canopy cover (Fig. 6D).

The potential impact of cool roof conversion and tree canopy expansion on *VE* in each 200 m grid cell, *i*, was estimated as

$$VE_{impact,i} = VE_{baseline,i} - VE_{roof/tree,i} \quad (4)$$

where VE_{roof} represents the VE under potential albedo conditions and VE_{tree} represents the VE under potential tree canopy cover conditions.

The cost of cool roof implementation per grid cell was estimated by multiplying the total albedo modified building area within the grid cell by the cost of \$69.97 m^{-2} as estimated by the city of Boston[39] to apply three applications of a light-colored coating, including additional costs associated with lifting materials, dumpsters, police details, and permits.

The cost of tree canopy expansion per grid cell was estimated by dividing the total area of modified tree cover per grid cell by 100 m^2, to estimate the number of trees required to produce the modified canopy cover area. The number of trees per grid cell was multiplied by the cost of \$2,023.70 estimated by the City of Boston[39] to plant a tree in an area that does not require a new tree pit, including additional costs of excavation, disposal, and soil mix. The unit costs used in this analysis represent average values reported by the City of Boston and likely vary on a case-by-case basis, such as cool roof installation requiring additional insulation or variable costs associated with different tree species and sizes. Additionally, the unit costs for Boston may not be representative of unit costs across other cities.

Constrained solution scenario
Despite the demonstrated interest of cities to incorporate cool roofs and tree canopy expansion to reduce heat exposure, budget constraints limit the extent to which solutions can be implemented. We explore a scenario to maximize heat exposure reduction by selecting the locations and types of intervention that provide the largest estimated *VE* reduction within a reasonable budget. We selected a budget corresponding to a one-time expenditure of \$34,080,037, which equals the City of Boston's Parks and Recreation Department's budget for fiscal year 2024 and represents 0.8% of the city operating budget. For all possible locations of tree canopy expansion and cool roof installation, estimated heat exposure impacts, defined as the potential reduction in *VE*, and costs for each intervention type per grid cell were compiled into a data table and sorted from highest impact to lowest impact. Using the sorted list of grid cells providing the highest impact, the cumulative cost of solutions for each grid cell was estimated until the budget was fully allocated. Grid cells and their corresponding solutions with a cumulative cost greater than the budget were removed from the dataset, yielding the locations and solutions shown in Fig. 4 estimated to provide the most heat exposure benefits within the budget.

Reporting summary
Further information on research design is available in the Nature Portfolio Reporting Summary linked to this article.

Data availability
Input data used in this analysis are publicly available at the following repositories: MADIS Air Temperature: https://madis-data.ncep.noaa.gov/madis_api.shtml. Sentinel-2 Reflectance: https://developers.google.com/earth-engine/datasets/catalog/COPERNICUS_S2_SR_HARMONIZED. Rapid Refresh Wind Speed: https://rapidrefresh.noaa.gov/. GOES-East Surface Solar Irradiance: https://osi-saf.eumetsat.int/products/osi-306-b. Daymet Air Temperature: https://daymet.ornl.gov/getdata. WorldPop Residential Population: https://developers.google.com/earth-engine/datasets/catalog/WorldPop_GP_100m_pop. CDC/ATSDR Social Vulnerability Index: https://www.atsdr.cdc.gov/place-health/php/svi/svi-data-documentation-download.html. The compiled weather station data for southern New England and population vulnerability data used in the analysis are available at the Harvard Dataverse: https://doi.org/10.7910/DVN/6FYMIE.

Code availability
The R code for the model fit and validation used in this manuscript is available at the Harvard Dataverse: https://doi.org/10.7910/DVN/6FYMIE.

References
1. Tuholske, C. et al. Global urban population exposure to extreme heat. *Proc. Natl. Acad. Sci.* **118**, e2024792118 (2021).
2. Mohajerani, A., Bakaric, J. & Jeffrey-Bailey, T. The urban heat island effect, its causes, and mitigation, with reference to the thermal properties of asphalt concrete. *J. Environ. Manag.* **197**, 522–538 (2017).
3. Ebi, K. L. et al. Hot weather and heat extremes: health risks. *Lancet* **398**, 698–708 (2021).
4. Liu, J. et al. Heat exposure and cardiovascular health outcomes: a systematic review and meta-analysis. *Lancet Planet. Health* **6**, e484–e495 (2022).
5. Colelli, F. P., Wing, I. S. & Cian, E. D. Air-conditioning adoption and electricity demand highlight climate change mitigation–adaptation tradeoffs. *Sci. Rep.* **13**, 4413 (2023).
6. Zhao, M., Lee, J. K. W., Kjellstrom, T. & Cai, W. Assessment of the economic impact of heat-related labor productivity loss: a systematic review. *Climatic Change* **167**, 22 (2021).
7. Chakraborty, T., Newman, A. J., Qian, Y., Hsu, A. & Sheriff, G. Residential segregation and outdoor urban moist heat stress disparities in the United States. *One Earth* **6**, 738–750 (2023).
8. Hsu, A., Sheriff, G., Chakraborty, T. & Manya, D. Disproportionate exposure to urban heat island intensity across major US cities. *Nat. Commun.* **12**, 2721 (2021).
9. Chakraborty, T., Venter, Z. S., Qian, Y. & Lee, X. Lower urban humidity moderates outdoor heat stress Chakraborty, T., Venter, Z. S., Qian, Y. & Lee, X. Lower Urban Humidity Moderates Outdoor Heat Stress. AGU Advances 3, e2022AV000729 (2022). *AGU Adv.* **3**, e2022AV000729 (2022).
10. Krayenhoff, E. S. et al. Cooling hot cities: a systematic and critical review of the numerical modelling literature. *Environ. Res. Lett.* **16**, 053007 (2021).
11. Santamouris, M. Cooling the cities—a review of reflective and green roof mitigation technologies to fight heat island and improve comfort in urban environments. *Sol. Energy* **103**, 682–703 (2014).
12. Smith, I. A., Fabian, M. P. & Hutyra, L. R. Urban green space and albedo impacts on surface temperature across seven United States cities. *Sci. Total Environ.* **857**, 159663 (2023).
13. Los Angeles County Department of Public Works Development Services Building and Safety Division. Cool Roof—Technical Requirements (2019).
14. City of Cambridge Department of Public Works. Tree Protection Ordinance Regulations (2021).
15. Rahman, M. A. et al. Tree cooling effects and human thermal comfort under contrasting species and sites. *Agric. For. Meteorol.* **287**, 107947 (2020).

16. Winbourne, J. B. et al. Tree transpiration and urban temperatures: current understanding, implications, and future research directions. *BioScience* **70**, 576–588 (2020).

17. Li, H. et al. Cooling efficacy of trees across cities is determined by background climate, urban morphology, and tree trait. *Commun. Earth Environ.* **5**, 754 (2024).

18. Du, M. et al. Daytime cooling efficiencies of urban trees derived from land surface temperature are much higher than those for air temperature. *Environ. Res. Lett.* **19**, 044037 (2024).

19. Ziter, C. D., Pedersen, E. J., Kucharik, C. J. & Turner, M. G. Scale-dependent interactions between tree canopy cover and impervious surfaces reduce daytime urban heat during summer. *Proc. Natl. Acad. Sci.* **116**, 7575–7580 (2019).

20. Trlica, A., Hutyra, L. R., Schaaf, C. L., Erb, A. & Wang, J. A. Albedo, land cover, and daytime surface temperature variation across an urbanized landscape. *Earth's. Future* **5**, 1084–1101 (2017).

21. Bruse, M. & Fleer, H. Simulating surface–plant–air interactions inside urban environments with a three dimensional numerical model. *Environ. Model. Softw.* **13**, 373–384 (1998).

22. Skamarock, C. et al. A description of the advanced research WRF Model Version 4.3 https://doi.org/10.5065/1dfh-6p97 (2021).

23. Schwaab, J. et al. The role of urban trees in reducing land surface temperatures in European cities. *Nat. Commun.* **12**, 6763 (2021).

24. Daly, C., Taylor, G. & Gibson, W. The prism approach to mapping precipitation and temperature (1997).

25. Thornton, M. M., Shrestha, R., Wei, Y., Thornton, P. E. & Kao, S.-C. Daymet: Daily Surface Weather Data on a 1-km Grid for North America, Version 4 R1. ORNL DAAC https://doi.org/10.3334/ORNLDAAC/2129 (2022).

26. Carrión, D. et al. A 1-km hourly air-temperature model for 13 northeastern U.S. states using remotely sensed and ground-based measurements. *Environ. Res.* **200**, 111477 (2021).

27. Ibsen, P. C., Jenerette, G. D., Dell, T., Bagstad, K. J. & Diffendorfer, J. E. Urban landcover differentially drives day and nighttime air temperature across a semi-arid city. *Sci. Total Environ.* **829**, 154589 (2022).

28. Centers for Disease Control and Prevention/ Agency for Toxic Substances and Disease Registry/ Geospatial Research, Analysis, and Services Program. CDC/ATSDR Social Vulnerability Index. https://www.atsdr.cdc.gov/placeandhealth/svi/data_documentation_download.html (2020).

29. Mohegh, A. et al. Observational Evidence of Neighborhood Scale Reductions in Air Temperature Associated with Increases in Roof Albedo. *Climate* **6**, 98 (2018).

30. Buzan, J. R. & Huber, M. Moist heat stress on a hotter Earth. *Annu. Rev. Earth Planet. Sci.* **48**, 623–655 (2020).

31. Zhang, K. et al. Increased heat risk in wet climate induced by urban humid heat. *Nature* **617**, 738–742 (2023).

32. Mueller, N. et al. Changing the urban design of cities for health: the superblock model. *Environ. Int.* **134**, 105132 (2020).

33. Bell Michelle, L., Gasparrini, A. & Benjamin Georges, C. Climate change, extreme heat, and health. *N. Engl. J. Med.* **390**, 1793–1801 (2024).

34. Hondula, D. M., Davis, R. E., Saha, M. V., Wegner, C. R. & Veazey, L. M. Geographic dimensions of heat-related mortality in seven U.S. cities. *Environ. Res.* **138**, 439–452 (2015).

35. Almanza, E., Jerrett, M., Dunton, G., Seto, E. & Ann Pentz, M. A study of community design, greenness, and physical activity in children using satellite, GPS and accelerometer data. *Health Place* **18**, 46–54 (2012).

36. Hartig, T., Mitchell, R., Vries, S. de & Frumkin, H. Nature and Health. *Annu. Rev. Public Health* **35**, 207–228 (2014).

37. Weinstein, N. et al. Seeing community for the trees: the links among contact with natural environments, community cohesion, and crime. *BioScience* **65**, 1141–1153 (2015).

38. Sproul, J., Wan, M. P., Mandel, B. H. & Rosenfeld, A. H. Economic comparison of white, green, and black flat roofs in the United States. *Energy Build.* **71**, 20–27 (2014).

39. City of Boston. Heat Resilience Solutions for Boston. (2022).

40. Bretz, S. E. & Akbari, H. Long-term performance of high-albedo roof coatings. *Energy Build.* **25**, 159–167 (1997).

41. Vogt, J., Hauer, R. J. & Fischer, B. C. The costs of maintaining and not maintaining the urban forest: a review of the urban forestry and arboriculture literature. *Arboric. Urban Forestry (AUF)* **41**, 293–323 (2015).

42. ENERGY STAR. ENERGY STAR® Program Requirements for Roof Products (2010).

43. Franceschi, E. et al. Crown shapes of urban trees-their dependences on tree species, tree age and local environment, and effects on ecosystem services. *Forests* **13**, 748 (2022).

44. Pretzsch, H. et al. Crown size and growing space requirement of common tree species in urban centres, parks, and forests. *Urban Forestry Urban Green.* **14**, 466–479 (2015).

45. Beck, H. E. et al. Present and future Köppen-Geiger climate classification maps at 1-km resolution. *Sci. Data* **5**, 180214 (2018).

46. Yang, L. et al. A new generation of the United States National Land Cover Database: requirements, research priorities, design, and implementation strategies. *ISPRS J. Photogramm. Remote Sens.* **146**, 108–123 (2018).

47. NCEP Meteorological Assimilation Data Ingest System (MADIS). https://madis.ncep.noaa.gov/.

48. Weather Underground. https://www.wunderground.com/.

49. A smoother ride and a more detailed Map thanks to AI. https://blog.google/products/maps/google-maps-101-ai-power-new-features-io-2021/.

50. Bonafoni, S. & Sekertekin, A. Albedo Retrieval From Sentinel-2 by New Narrow-to-Broadband Conversion Coefficients. *IEEE Geosci. Remote Sens. Lett.* **17**, 1618–1622 (2020).

51. Benjamin, S. G. et al. A North American Hourly assimilation and model forecast cycle: the rapid refresh. (2016) https://doi.org/10.1175/MWR-D-15-0242.1.

52. OSI SAF GOES-East Surface Solar Irradiance. EUMETSAT Ocean and Sea Ice Satellite Application Facility https://osi-saf.eumetsat.int/products/osi-306-b (2021).

53. R Core Team. *R: A Language and Environment for Statistical Computing* (The R Foundation for Statistical Computing (2023).

54. Tieskens, K. F., Smith, I. A., Jimenez, R. B., Hutyra, L. R. & Fabian, M. P. Mapping the gaps between cooling benefits of urban greenspace and population heat vulnerability. *Sci. Total Environ.* **845**, 157283 (2022).

55. Sorichetta, A. et al. High-resolution gridded population datasets for Latin America and the Caribbean in 2010, 2015, and 2020. *Sci. Data* **2**, 150045 (2015).

56. Pavanello, F. et al. Air-conditioning and the adaptation cooling deficit in emerging economies. *Nat. Commun.* **12**, 6460 (2021).

57. Popp, Z., Sue Wing, I., Lane, K. J. & Wellenius, G. A. A US heat disaster? Intersection of social vulnerability and temperature extremes exacerbated by mid-century climate change and population shifts. *Environ. Res.: Health* **3**, 025009 (2025).

58. City of Boston. Boston Buildings Inventory. Analyze Boston https://data.boston.gov/dataset/boston-buildings-inventory (2020).

59. City of Boston. Property Assessment. Analyze Boston https://data.boston.gov/dataset/property-assessment (2020).

60. City of Boston. Treekeeper Street Trees. Analyze Boston https://data.boston.gov/dataset/treekeeper-street-trees (2024).

Acknowledgements

Author contributions

I.A.S. and L.R.H. conceptualized the research and designed the study, with contributions from D.L., D.K.F., G.A.W. I.A.S. processed data, generated results, and conducted analyses. D.L., D.K.F., G.A.W. and L.R.H. reviewed results and analyses. I.A.S. and L.R.H. led the writing of the manuscript, with all authors contributing editorially.

Competing interests

The authors declare the following competing interests: GAW currently serves as a consultant for the Health Effects Institute (Boston, MA) and recently served as a consultant for Google, LLC (Mountain View, CA).

Additional information

Supplementary information The online version contains supplementary material available at https://doi.org/10.1038/s43247-025-02462-3.

Correspondence and requests for materials should be addressed to Ian A. Smith.

Peer review information *Communications Earth and Environment* thanks Siqi Jia, Jiwei Zou and the other, anonymous, reviewer(s) for their contribution to the peer review of this work. Primary Handling Editors: Charlotte Kendra Gotangco Gonzales and Aliénor Lavergne. [A peer review file is available.]

Reprints and permissions information is available at http://www.nature.com/reprints

Publisher's note Springer Nature remains neutral with regard to jurisdictional claims in published maps and institutional affiliations.